Comp2Comp: Open-Source Body Composition Assessment on Computed Tomography

Author name(s) withheld EMAIL(S) WITHHELD
Address withheld

Editors: Under Review for MIDL 2023

Abstract

Computed tomography (CT) can provide quantitative body composition metrics of tissue volume, morphology, and quality which are valuable for disease prediction and prognostication. However, manually extracting these measures is a cumbersome and time-consuming task. Proprietary software to automate this process exist, but these software are closed-source, impeding large-scale access to and usage of these tools. To address this, we have built `Comp2Comp`, an open-source Python package for rapid and automated body composition analysis of CT scans. The primary advantages of `Comp2Comp` are its open-source nature, the inclusion of multiple tissue analysis capabilities within a single package, and its extensible design. We discuss the architecture of `Comp2Comp` and report initial validation results. `Comp2Comp` can be found at `https://github.com/StanfordMIMI/Comp2Comp`.

Keywords: computed tomography, segmentation, body composition, abdominal CT.

1. Introduction

Quantitative metrics from computed tomography (CT) can provide diagnostic and prognostic biomarkers for acute and chronic health conditions (Lee et al., 2022a; Thibault et al., 2012; Kuriyan, 2018). Such measures can provide a more objective evaluation of body composition (BC) than traditional clinical measurements (e.g. weight, body mass index (BMI), waist circumference, skinfolds) (Zeng et al., 2021). However, manually extracting quantitative BC measures from CT scans is time-consuming and prone to inter-reader variability, which considerably limits their utility in clinics and research studies.

We introduce `Comp2Comp`, an open-source Python package to expedite CT-based BC analysis. `Comp2Comp` contains methods to automatically segment CT images, extract quantitative BC measures, and generate polychromatic visual reports. `Comp2Comp` is designed to be extensible, enabling the development of complex clinically-relevant applications. The package is hosted on the GitHub platform at `https://github.com/StanfordMIMI/Comp2Comp` with a permissive license.

2. Inference Pipelines

A key component of `Comp2Comp` is its inference pipeline system. Inference pipelines string together sequences of building-block inference class modules which perform specific tasks like machine learning, saving or loading data, visualizing outputs, or other computational tasks. Furthermore, inference pipelines can be reused within other inference pipelines. This modular structure shortens iteration cycles for developing complex clinical applications. We list the pipelines currently implemented in `Comp2Comp`. Each of these pipelines saves numerical or categorical results, image reports, and segmentation files. All trained models are available on HuggingFace and downloaded automatically within `Comp2Comp`.

© 2023 CC-BY 4.0, Anonymous.

2.1. Spine Bone Mineral Density from 3D Trabecular Bone Regions at T12-L5

Retrospective studies have established that L1 trabecular bone density of < 90 Hounsfield units (HU) is associated with a high risk of vertebral fracture (odds ratio, 32) (Graffy et al., 2017; Lee et al., 2018). Large scale screening for osteoporosis using CT has been validated in retrospective cohorts (Roux et al., 2022; Pickhardt et al., 2020), but is not yet widely implemented because automated techniques have not been freely disseminated.

We provide options for running the TotalSegmentator (TS) spine model (Wasserthal et al., 2022) as well as an nnUNet trained on VerSe (Sekuboyina et al., 2021; Löffler et al., 2020; Liebl et al., 2021) and TS data (Wasserthal et al., 2022). We develop heuristics for extracting 3D regions of interest (ROIs) from vertebral body trabecular bone as described previously (Blankemeier et al., 2023). `Comp2Comp` reports average HUs within these ROIs.

We validate our method with TS on 40 contrast-enhanced CT scans from the Stanford emergency department. Comparing to central regions extracted from labeled T12-L5 vertebral bodies, we achieve an average HU percent error of 1.82±0.86 across these 6 levels.

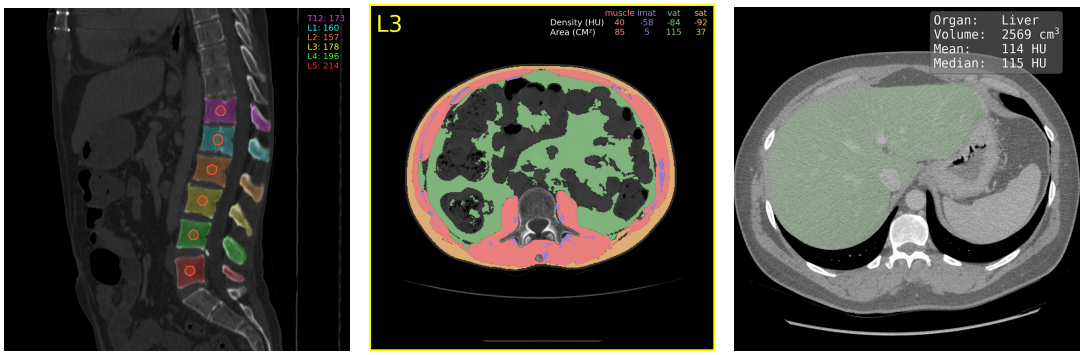

(a) (b) (c)

Figure 1: (a) Curved planar projection from our spine inference pipeline. Within the image, we report average ROI HU at T12-L5. (b) Output image from our spine, muscle, and adipose tissue pipeline. Here, the level is automatically determined using the spine model. Within the image, we report mean HU and area of each segmented tissue. (c) Output image from our liver, spleen, and pancreas inference pipeline. Within the image, we report the organ volume, as well as mean and median HU.

2.2. Slice-by-Slice 2D Analysis of Muscle and Adipose Tissue

Sarcopenia, defined by the loss of muscle tissue and muscle function, is associated with adverse outcomes, such as post-operative complications (Papadopoulou et al., 2020; Surov and Wienke, 2022). Adipose tissue, particularly visceral adipose tissue (VAT), is a modifiable risk factor for numerous medical conditions (Vilalta et al., 2022; Rao et al., 2021; Katzmarzyk et al., 2022).

We provide two models for 2D segmentation of muscle and adipose tissue. Both are 2D UNet models trained on axial CT slices at the L3 vertebral level.

On an internal test set of 40 abdominal contrast-enhanced cases at the L3 vertebral level, we achieve the following mean (standard deviation) Dice scores: 0.97 (0.03), 0.96 (0.05), and 0.97 (0.02) for muscle, VAT, and subcutaneous adipose tissue (SAT) respectively. The error in HU and area averaged below 1% and 2%, respectively, for all tissues. For the same three tissues, we achieve 94.7 (5.9), 94.6 (6.7), and 93.2 (14.8) on 20 external cases.

2.3. Contrast Phase Detection

Contrast agents are used to enhance the radiodensity of the blood vessels and vascularized tissues. Determining contrast phase is an important step for the successful application of algorithms with outputs that are sensitive to pixel intensity.

The `Comp2Comp` contrast phase detection pipeline consists of segmenting key anatomical structures, extracting metrics from these structures, and classifying these into one of 4 classes (non-contrast, arterial, venous and delayed) using a gradient boosting classifier.

On 362 internal test cases, our method achieves F1 scores of 0.96, 0.78, 0.92, and 0.95 for non-contrast, arterial, venous, and delayed phases respectively.

2.4. 3D Analysis of Liver, Spleen, and Pancreas

Liver disease and cirrhosis, the ninth leading cause of death, can be predicted by the volume, morphology, and attenuation of liver and spleen structures (Lee et al., 2022b). Volume measures can identify enlarged organs and aid in transplant planning (Linguraru et al., 2010).

`Comp2Comp` provides 3D analyses of the liver, spleen and pancreas. The volume, as well as the mean and median HU intensities are recorded. The organ segmentations are displayed in the axial and coronal planes. The slice with the largest cross-sectional area is displayed in the axial plane and the slice with the longest continuous length is displayed in the coronal plane. To segment these organs, we leverage TS (Wasserthal et al., 2022).

2.5. Combining Inference Pipelines: End-to-End Spine, Muscle, and Adipose Tissue Analysis at T12-L5

The modular design of `Comp2Comp` makes it easy to combine various `Comp2Comp` inference pipelines. Our spine, muscle, and adipose tissue pipeline combines the spine pipeline with the muscle and adipose tissue pipeline to analyze spine bone mineral density, muscle and adipose tissue at T12-L5.

To select the axial slices for muscle and adipose tissue segmentation, we compute per-level superior/inferior (SI) centers. Comparing to SI centers from our labeled T12-L5 vertebral bodies, we achieve an average error of 4.2$\pm$2.0mm across T12-L5. On 20 external cases, our segmentation model achieves mean (standard deviation) Dice scores, averaged across T12-L5, of: 0.88 (0.08), 0.93 (0.07), 0.91 (0.16) for muscle, VAT, and SAT respectively.

3. Conclusion

We present C2C, a tool for automated analysis of multiple tissues that is extensible and open source. We hope that `Comp2Comp` will increase the usage of BC analysis in large-scale research studies and clinical settings. We welcome any contributions from the community.

References

Louis Blankemeier, Arjun Desai, Juan Manuel Zambrano Chaves, Andrew Wentland, Sally Yao, Eduardo Reis, Malte Jensen, Bhanushree Bahl, Khushboo Arora, Bhavik N Patel, et al. Comp2comp: Open-source body composition assessment on computed tomography. *arXiv preprint arXiv:2302.06568*, 2023.

Peter M Graffy, Scott J Lee, Timothy J Ziemlewicz, and Perry J Pickhardt. Prevalence of vertebral compression fractures on routine ct scans according to l1 trabecular attenuation: determining relevant thresholds for opportunistic osteoporosis screening. *American Journal of Roentgenology*, 209(3):491–496, 2017.

Peter T Katzmarzyk, Justin C Brown, Shengping Yang, Emily F Mire, Xiao-Cheng Wu, Lucio Miele, Augusto C Ochoa, and Jovanny Zabaleta. Association of abdominal visceral adiposity and total fat mass with cancer incidence and mortality in white and black adults. *Cancer Epidemiology, Biomarkers & Prevention*, 31(8):1532–1538, 2022.

Rebecca Kuriyan. Body composition techniques. *The Indian journal of medical research*, 148(5):648, 2018.

Matthew H Lee, Ryan Zea, John W Garrett, Peter M Graffy, Ronald M Summers, and Perry J Pickhardt. Abdominal ct body composition thresholds using automated ai tools for predicting 10-year adverse outcomes. *Radiology*, page 220574, 2022a.

Scott J Lee, Peter M Graffy, Ryan D Zea, Timothy J Ziemlewicz, and Perry J Pickhardt. Future osteoporotic fracture risk related to lumbar vertebral trabecular attenuation measured at routine body ct. *Journal of Bone and Mineral Research*, 33(5):860–867, 2018.

Sungwon Lee, Daniel C Elton, Alexander H Yang, Christopher Koh, David E Kleiner, Meghan G Lubner, Perry J Pickhardt, and Ronald M Summers. Fully automated and explainable liver segmental volume ratio and spleen segmentation at ct for diagnosing cirrhosis. *Radiology: Artificial Intelligence*, 4(5):e210268, 2022b.

Hans Liebl, David Schinz, Anjany Sekuboyina, Luca Malagutti, Maximilian T Löffler, Amirhossein Bayat, Malek El Husseini, Giles Tetteh, Katharina Grau, Eva Niederreiter, et al. A computed tomography vertebral segmentation dataset with anatomical variations and multi-vendor scanner data. *Scientific Data*, 8(1):284, 2021.

Marius George Linguraru, Jesse K Sandberg, Zhixi Li, Furhawn Shah, and Ronald M Summers. Automated segmentation and quantification of liver and spleen from ct images using normalized probabilistic atlases and enhancement estimation. *Medical physics*, 37 (2):771–783, 2010.

Maximilian T Löffler, Anjany Sekuboyina, Alina Jacob, Anna-Lena Grau, Andreas Scharr, Malek El Husseini, Mareike Kallweit, Claus Zimmer, Thomas Baum, and Jan S Kirschke. A vertebral segmentation dataset with fracture grading. *Radiology: Artificial Intelligence*, 2(4):e190138, 2020.

SK Papadopoulou, P Tsintavis, G Potsaki, and Dimitrios Papandreou. Differences in the prevalence of sarcopenia in community-dwelling, nursing home and hospitalized individuals. a systematic review and meta-analysis. *The journal of nutrition, health & aging*, 24:83–90, 2020.

Perry J Pickhardt, Peter M Graffy, Ryan Zea, Scott J Lee, Jiamin Liu, Veit Sandfort, and Ronald M Summers. Automated abdominal ct imaging biomarkers for opportunistic prediction of future major osteoporotic fractures in asymptomatic adults. *Radiology*, 297 (1):64–72, 2020.

Vishal N Rao, Christopher G Bush, Morgana Mongraw-Chaffin, Michael E Hall, Donald Clark III, Marat Fudim, Adolfo Correa, Bradley G Hammill, Emily O'Brien, Yuan-I Min, et al. Regional adiposity and risk of heart failure and mortality: the jackson heart study. *Journal of the American Heart Association*, 10(14):e020920, 2021.

Christian Roux, Antoine Rozes, Daniel Reizine, David Hajage, Christel Daniel, Aurélien Maire, Stéphane Bréant, Namik Taright, Ronen Gordon, Jacques Fechtenbaum, et al. Fully automated opportunistic screening of vertebral fractures and osteoporosis on more than 150 000 routine computed tomography scans. *Rheumatology*, 61(8):3269–3278, 2022.

Anjany Sekuboyina, Malek E Husseini, Amirhossein Bayat, Maximilian Löffler, Hans Liebl, Hongwei Li, Giles Tetteh, Jan Kukačka, Christian Payer, Darko Štern, et al. Verse: A vertebrae labelling and segmentation benchmark for multi-detector ct images. *Medical image analysis*, 73:102166, 2021.

Alexey Surov and Andreas Wienke. Prevalence of sarcopenia in patients with solid tumors: A meta-analysis based on 81,814 patients. *Journal of Parenteral and Enteral Nutrition*, 46(8):1761–1768, 2022.

Ronan Thibault, Laurence Genton, and Claude Pichard. Body composition: why, when and for who? *Clinical nutrition*, 31(4):435–447, 2012.

Adrian Vilalta, Julio A Gutiérrez, SuZanne Chaves, Moisés Hernández, Silvia Urbina, and Marcus Hompesch. Adipose tissue measurement in clinical research for obesity, type 2 diabetes and nafld/nash. *Endocrinology, Diabetes & Metabolism*, 5(3):e00335, 2022.

Jakob Wasserthal, Manfred Meyer, Hanns-Christian Breit, Joshy Cyriac, Shan Yang, and Martin Segeroth. Totalsegmentator: robust segmentation of 104 anatomical structures in ct images. *arXiv preprint arXiv:2208.05868*, 2022.

Qiang Zeng, Ling Wang, Shengyong Dong, Xiaojuan Zha, Limei Ran, Yongli Li, Shuang Chen, Jianbo Gao, Shaolin Li, Yong Lu, et al. Ct-derived abdominal adiposity: Distributions and better predictive ability than bmi in a nationwide study of 59,429 adults in china. *Metabolism*, 115:154456, 2021.